fractal and fractional

MDPI

Article

A Comparative Study of Responses of Fractional Oscillator to Sinusoidal Excitation in the Weyl and Caputo Senses

Jun-Sheng Duan [1], Yu-Jie Lan [1] and Ming Li [2,3,*]

[1] School of Sciences, Shanghai Institute of Technology, Shanghai 201418, China
[2] Ocean College, Zhejiang University, Zhoushan 316021, China
[3] Village 1, East China Normal University, Shanghai 200062, China
* Correspondence: mli15@zju.edu.cn or mli@ee.ecnu.edu.cn

Abstract: The fractional oscillator equation with the sinusoidal excitation $mx''(t) + b\,D_t^{\alpha}x(t) + kx(t) = F\sin(\omega t)$, $m, b, k, \omega > 0$ and $0 < \alpha < 2$ is comparatively considered for the Weyl fractional derivative and the Caputo fractional derivative. In the sense of Weyl, the fractional oscillator equation is solved to be a steady periodic oscillation $x_W(t)$. In the sense of Caputo, the fractional oscillator equation is solved and subjected to initial conditions. For the fractional case $\alpha \in (0,1) \cup (1,2)$, the response to excitation, $S(t)$, is a superposition of three parts: the steady periodic oscillation $x_W(t)$, an exponentially decaying oscillation and a monotone recovery term in negative power law. For the two responses to initial values, $S_0(t)$ and $S_1(t)$, either of them is a superposition of an exponentially decaying oscillation and a monotone recovery term in negative power law. The monotone recovery terms come from the Hankel integrals which make the fractional case different from the integer-order case. The asymptotic behaviors of the solutions removing the steady periodic response are given for the four cases of the initial values. The Weyl fractional derivative is suitable for a describing steady-state problem, and can directly lead to a steady periodic solution. The Caputo fractional derivative is applied to an initial value problem and the steady component of the solution is just the solution in the corresponding Weyl sense.

Keywords: fractional calculus; fractional oscillator; Weyl fractional derivative; Caputo fractional derivative; Laplace transform

Citation: Duan, J.-S.; Lan, Y.-J.; Li, M. A Comparative Study of Responses of Fractional Oscillator to Sinusoidal Excitation in the Weyl and Caputo Senses. *Fractal Fract.* **2022**, *6*, 692. https://doi.org/10.3390/fractalfract6120692

Academic Editors: Salah Mahmoud Boulaaras, Viet-Thanh Pham and Rashid Jan

Received: 18 October 2022
Accepted: 19 November 2022
Published: 23 November 2022

Publisher's Note: MDPI stays neutral with regard to jurisdictional claims in published maps and institutional affiliations.

1. Introduction

Fractional calculus has been attracting significant attention in recent decades since it can be used to describe the memory and hereditary properties of various materials and processes [1–9]. Its application fields are extensive, including viscoelastic a constitutive relationship [4,7,10], anomalous diffusion [2,4], vibration and relaxation [2,4,7,8], control theory [2,5], stochastic process [11,12], etc.

Let $f(t)$ be integrable on any finite subinterval of $(a, +\infty)$. Then, the Riemann–Liouville fractional integral of $f(t)$ of order ν is defined as

$$J_{a,t}^{\nu} f(t) = \int_a^t \frac{(t-\tau)^{\nu-1}}{\Gamma(\nu)} f(\tau)d\tau,\ t > a, \tag{1}$$

for $\nu > 0$, and $J_{a,t}^{0} f(t) = f(t)$ for $\nu = 0$, where $\Gamma(\cdot)$ is the gamma function.

Let α be a real positive number, $m - 1 < \alpha \le m$, $m \in \mathbb{N}$, and the function $f(t)$ has an absolutely continuous $(m-1)$st derivative on any finite subinterval of $(a, +\infty)$. Then, the Riemann–Liouville fractional derivative of $f(t)$ of order α is defined as

$${}^{RL}D_{a,t}^{\alpha} f(t) = \frac{d^m}{dt^m}\left(J_{a,t}^{m-\alpha} f(t)\right),\ t > a, \tag{2}$$

while the Caputo fractional derivative of $f(t)$ of order α is defined as

$$ {}^{C}D^{\alpha}_{a,t}f(t) = J^{m-\alpha}_{a,t}\left(f^{(m)}(t)\right),\ t > a. \tag{3}$$

Usually, a is a finite number and without loss of generality, a is taken as 0. If we choose $a = -\infty$, then the operator in (1) is known as the Weyl fractional integral, while the operator in (2) or (3), which are consistent in this case, is known as the Weyl fractional derivative [13]. Theoretical analyses and experimental simulations have indicated that the stress–strain relationship of a viscoelastic body can be better described by introducing the fractional calculus, such as the Scott–Blair model [4], the Kelvin–Voigt, Maxwell and Zener models [4,10,14], among others [7,15,16]. Thus, vibration problems involving a viscoelastic medium with a fractional stress–strain relationship lead to fractional oscillator equations [7,8,17–25].

In [22], fractional oscillator equations in the sense of the Weyl fractional calculus were clarified and analyzed. In [11], the fractional oscillator was described by a stochastic differential equation with the Weyl fractional calculus. In [26,27], the Weyl fractional derivative was used to derive the steady response of a fractional oscillator system. Comparatively, the Caputo fractional derivative is more commonly used in modeling physical or mechanical problems partly due to the feasible classical initial conditions [4,7,9,19–21,24,28]. The objective of this paper was to understand the differences and relationship between the Weyl fractional derivative and the Caputo fractional derivative in modeling the fractional oscillator equations. By imposing the sinusoidal excitation, we derive the steady periodic response for the Weyl case, while an initial value problem needs to be solved for the Caputo case. We will show that the steady component of the response for the Caputo case is just the response for the corresponding Weyl case.

For short, we used ${}^{W}D^{\alpha}_{t}f(t)$ to denote the Weyl fractional derivative ${}^{RL}D^{\alpha}_{-\infty,t}f(t)$ or ${}^{C}D^{\alpha}_{-\infty,t}f(t)$, and ${}^{C}D^{\alpha}_{t}f(t)$ the Caputo fractional derivative ${}^{C}D^{\alpha}_{0,t}f(t)$. For the model based on the Caputo fractional derivative, we will use the Laplace transform

$$ \tilde{f}(s) = \mathcal{L}[f(t)] = \int_0^{+\infty} f(t)e^{-st}dt \tag{4}$$

and its complex inverse integral formula

$$ f(t) = \mathcal{L}^{-1}\left[\tilde{f}(s)\right] = \frac{1}{2\pi \mathrm{i}}\int_{\mathrm{Br}} \tilde{f}(s)e^{st}ds, \tag{5}$$

and the Laplace transform formula of the Caputo fractional derivative

$$ \mathcal{L}\left[{}^{C}D^{\alpha}_{t}f(t)\right] = s^{\alpha}\tilde{f}(s) - \sum_{k=0}^{m-1} f^{(k)}(0)s^{\alpha-1-k},\ m-1 < \alpha \le m. \tag{6}$$

In this paper, we consider the response of the fractional oscillator to sinusoidal excitation. In the next Section 2, the fractional derivative is in the sense of Weyl and a steady periodic response is directly obtained by the method of undetermined coefficients. In Section 3, the fractional derivative is in the sense of Caputo and an initial value problem needs to be solved. The response is much more complicated than the Weyl case, and is solved in detail using the Laplace transform and its complex inverse integral formula. A comparative study of the responses of fractional oscillator in the Weyl and Caputo senses is conducted. Section 4 summarizes our conclusions.

2. Oscillator Equation with the Weyl Fractional Derivative

Consider the fractional oscillator equation with the Weyl fractional derivative and the sinusoidal excitation

$$ mx''(t) + b({}^{W}D^{\alpha}_{t}x(t)) + kx(t) = F\sin(\omega t),\ m, b, k, \omega > 0, \tag{7}$$

where F is a constant and the order α is limited in the interval $0 < \alpha < 2$.

Suppose the response has the amplitude X and phase lag ψ,

$$x(t) = X\sin(\omega t - \psi), \tag{8}$$

then the Weyl fractional derivative is [13]

$${}^{W}D_t^{\alpha}x(t) = X\omega^{\alpha}\sin\Big(\omega t - \psi + \frac{\alpha\pi}{2}\Big). \tag{9}$$

Substituting into (7) and equating the coefficients of $\sin(\omega t)$ and $\cos(\omega t)$, respectively, on both sides, we obtain

$$\begin{aligned} X(k - m\omega^2)\cos(\psi) + bX\omega^{\alpha}\cos\Big(\frac{\alpha\pi}{2} - \psi\Big) &= F, \\ (k - m\omega^2)\sin(\psi) - b\omega^{\alpha}\sin\Big(\frac{\alpha\pi}{2} - \psi\Big) &= 0. \end{aligned}$$

Furthermore, the amplitude and phase lag are solved as

$$X = \frac{F}{\sqrt{\big(k - m\omega^2 + b\omega^{\alpha}\cos\big(\frac{\alpha\pi}{2}\big)\big)^2 + \big(b\omega^{\alpha}\sin\big(\frac{\alpha\pi}{2}\big)\big)^2}}, \tag{10}$$

$$\tan(\psi) = \frac{b\omega^{\alpha}\sin\big(\frac{\alpha\pi}{2}\big)}{k - m\omega^2 + b\omega^{\alpha}\cos\big(\frac{\alpha\pi}{2}\big)}, \tag{11}$$

where the phase lag is limited to the interval $0 \le \psi < \pi$. Thus, the steady periodic response is derived as

$$x_W(t) = \frac{F\sin(\omega t - \psi)}{\sqrt{\big(k - m\omega^2 + b\omega^{\alpha}\cos\big(\frac{\alpha\pi}{2}\big)\big)^2 + \big(b\omega^{\alpha}\sin\big(\frac{\alpha\pi}{2}\big)\big)^2}}, \tag{12}$$

where the subscript W denotes the solution for Equation (7) with the Weyl fractional derivative. The response is a sinusoidal oscillation with same frequency as the excitation with frequency-dependent amplitude and phase lag.

We look into the amplitude ratio

$$\beta(\omega) = \frac{X}{F/k} = \frac{k}{\sqrt{\big(k - m\omega^2 + b\omega^{\alpha}\cos\big(\frac{\alpha\pi}{2}\big)\big)^2 + \big(b\omega^{\alpha}\sin\big(\frac{\alpha\pi}{2}\big)\big)^2}}, \tag{13}$$

and the phase lag $\psi(\omega)$ as functions of the excitation frequency ω. It is obvious that $\beta(\omega) \to 1$ as $\omega \to 0^+$. The derivative of amplitude ratio $\beta(\omega)$ satisfies

$$\beta'(\omega) \sim -\alpha b k^{-1}\cos\Big(\frac{\alpha\pi}{2}\Big)\omega^{\alpha-1},\ \omega \to 0^+.$$

Thus, the limit as $\omega \to 0^+$ is

$$\beta'(0^+) = \begin{cases} 0, & 1 \le \alpha < 2, \\ -\infty, & 0 < \alpha < 1. \end{cases} \tag{14}$$

The amplitude–frequency curves $\beta(\omega)$ vs. ω are plotted in Figure 1 for $m = 1$, $b = 2$, $k = 3$ and $\alpha = 0.3, 0.65, 1, 1.35, 1.7$. The plot of the phase lag $\psi(\omega)$ vs. ω is shown in Figure 2 for the same parameter values. The amplitude–frequency curve in Figure 1 displays a decreasing initial passage for the case of $0 < \alpha < 1$. For the two limiting cases $\alpha = 0$ and $\alpha = 2$, the undamped natural frequencies are $\sqrt{(k+b)/m} = \sqrt{5}$ and $\sqrt{k/(m+b)} = 1$. The resonant frequency in Figure 1 shifts to them nearby as α is close to the two endpoints 0 and 2. As α approaches to 1, the format becomes low and a large damping is implied. The

fractional case exhibits a stronger resonance phenomenon than the case of $\alpha = 1$. Figure 2 displays the transition process of the phase lag $\psi(\omega)$ with ω. The transition happens around the resonant frequency. As α approaches towards 1, the transition becomes gentle.

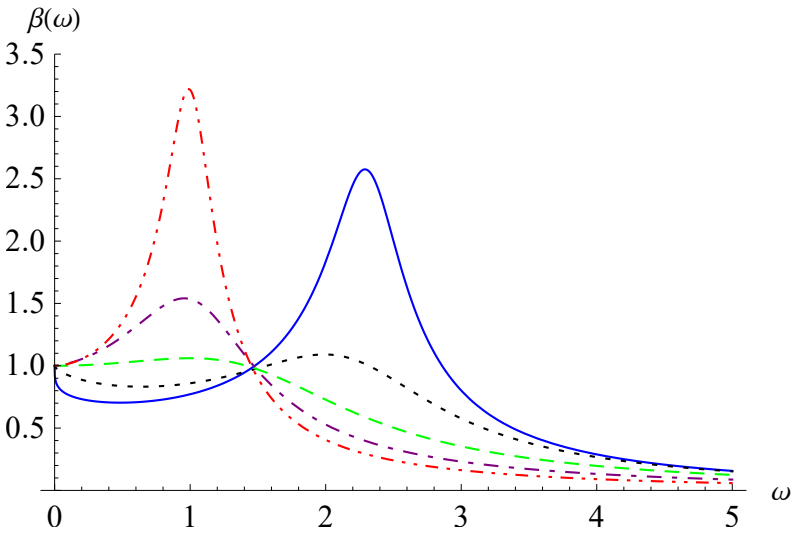

Figure 1. Curves of amplitude ratio $\beta(\omega) = Xk/F$ for $m = 1, b = 2, k = 3$ and $\alpha = 0.3$ (solid line), $\alpha = 0.65$ (dot line), $\alpha = 1$ (dash line), $\alpha = 1.35$ (dot–dash line), $\alpha = 1.7$ (dot–dot–dash line).

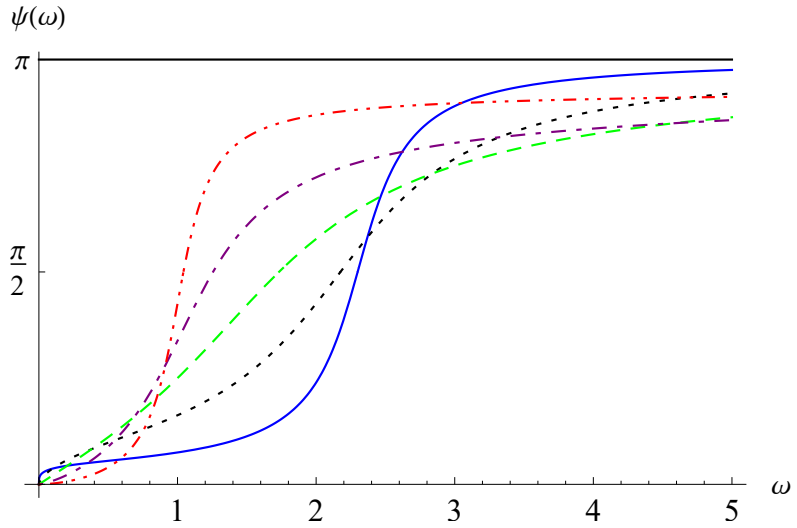

Figure 2. Curves of phase lag $\psi(\omega)$ for $m = 1, b = 2, k = 3$ and $\alpha = 0.3$ (solid line), $\alpha = 0.65$ (dot line), $\alpha = 1$ (dash line), $\alpha = 1.35$ (dot–dash line), $\alpha = 1.7$ (dot–dot–dash line).

3. Oscillator Equation with the Caputo Fractional Derivative

Consider the fractional oscillator equation with the Caputo fractional derivative and the sinusoidal excitation

$$mx''(t) + b({}^{C}D_t^{\alpha}x(t)) + kx(t) = F\sin(\omega t),\ m, b, k, \omega > 0, \tag{15}$$

$$x(0) = x_0,\ x'(0) = x_1, \tag{16}$$

where F is a constant, x_0 and x_1 are specified initial values and the order α satisfies $0 < \alpha < 2$.

Operating the Laplace transform to Equation (15) with the initial condition (16) gives

$$m(s^2\tilde{x}(s) - sx_0 - x_1) + b(s^{\alpha}\tilde{x}(s) - s^{\alpha-1}x_0 - \lceil \alpha - 1 \rceil s^{\alpha-2}x_1) + k\tilde{x}(s) = \frac{F\omega}{s^2 + \omega^2}.$$

where $\tilde{x}(s) = \mathcal{L}[x(t)]$ is the Laplace transform of $x(t)$, for $\alpha \neq 1$, the one-valued branch $s^\alpha = e^{\alpha(\ln|s|+\mathrm{i}\arg s)}$, $-\pi < \arg s < \pi$, is taken, and $\lceil \alpha - 1 \rceil$ denotes the least integer no less than $\alpha - 1$. Thus, if $0 < \alpha \leq 1$, then $\lceil \alpha - 1 \rceil = 0$, and if $1 < \alpha < 2$, then $\lceil \alpha - 1 \rceil = 1$. Like an integer-order equation, refer to the trinomial

$$C(s) = ms^2 + bs^\alpha + k, \tag{17}$$

as the characteristic polynomial with a fractional power. As such, the Laplace image function has the expression

$$\tilde{x}(s) = \frac{F\omega}{(s^2+\omega^2)C(s)} + x_0\frac{ms + bs^{\alpha-1}}{C(s)} + x_1\frac{m + \lceil \alpha - 1 \rceil bs^{\alpha-2}}{C(s)}.$$

We introduce three special responses, i.e., the response to excitation and the two responses to initial values,

$$S(t) = F\omega\mathcal{L}^{-1}\left[\frac{1}{(s^2+\omega^2)C(s)}\right], \tag{18}$$

$$S_0(t) = x_0\mathcal{L}^{-1}\left[\frac{ms + bs^{\alpha-1}}{C(s)}\right], \tag{19}$$

$$S_1(t) = x_1\mathcal{L}^{-1}\left[\frac{m + \lceil \alpha - 1 \rceil bs^{\alpha-2}}{C(s)}\right]. \tag{20}$$

Thus, the solution is a superposition of them

$$x(t) = S(t) + S_0(t) + S_1(t). \tag{21}$$

In order to obtain results that are convenient to compare with those in last section, we consider the inverses in (18)–(20) by using the complex inverse integral formula, e.g., for (18), the formula reads

$$S(t) = \frac{F\omega}{2\pi\mathrm{i}}\int_{\mathrm{Br}}\frac{e^{st}}{(s^2+\omega^2)C(s)}ds, \tag{22}$$

where Br denotes the Bromwich path, i.e., a straight-line $\mathrm{Re}(s) = \gamma > 0$. The poles of the integrand from the sinusoidal excitation are two purely imaginary numbers and denoted by

$$s_{1,2} = \pm\mathrm{i}\omega.$$

If $\alpha = 1$, then the power function s^α is a single-valued holomorphic function on the whole complex plane, while if $\alpha \in (0,1) \cup (1,2)$, the function s^α has a branch cut, which is taken as the nonpositive real axis here. Moreover, for a distribution of zeros of $C(s)$, the fractional case is different from the integer-order case. Accordingly, we solve the problem separately in the two following subsections in a contrasting way.

3.1. The Integer-Order Case $\alpha = 1$

The integral in (22) can be reduced from the loop integral on the contour shown in Figure 3. By the residue theorem and Jordan's lemma, Equation (22) is expressed as a sum of residues of the integrand. The singularities comprise the poles from the sinusoidal excitation, $s_{1,2} = \pm\mathrm{i}\omega$ and the poles from the characteristic polynomial

$$C(s) = ms^2 + bs + k.$$

We denote the residue contributions from the two types of poles by $S_{RE}(t)$ and $S_{RC}(t)$, respectively. Thus, we have

$$\begin{aligned} S(t) &= S_{RE}(t) + S_{RC}(t) \\ &= F\omega \sum_{i=1}^{2} \mathrm{Res}\left(\frac{e^{st}}{(s^2+\omega^2)C(s)}, s_i \right) + F\omega \sum_{i} \mathrm{Res}\left(\frac{e^{st}}{(s^2+\omega^2)C(s)}, s_i \right), \end{aligned} \tag{23}$$

where the s_i in the second sum are poles from the characteristic polynomial $C(s)$ and have negative real parts. By calculating the residues at the two simple poles $s_{1,2}$ we obtain $S_{RE}(t)$ as follows and it is just the special case of $x_W(t)$ as $\alpha = 1$ in Section 2,

$$\begin{aligned} S_{RE}(t) &= F\omega \left(\frac{e^{s_1 t}}{2s_1 C(s_1)} + \frac{e^{s_2 t}}{2s_2 C(s_2)} \right) \\ &= \frac{F\big((k - m\omega^2)\sin(\omega t) - b\omega\cos(\omega t) \big)}{(k-m\omega^2)^2 + (b\omega)^2} = x_W(t; \alpha = 1). \end{aligned} \tag{24}$$

For $S_0(t)$ and $S_1(t)$ in (19) and (20), we derive in a similar manner that

$$S_0(t) = x_0 \mathcal{L}^{-1}\left[\frac{ms+b}{C(s)} \right] = x_0 \sum_i \mathrm{Res}\left(\frac{(ms+b)e^{st}}{C(s)}, s_i \right), \tag{25}$$

$$S_1(t) = x_1 \mathcal{L}^{-1}\left[\frac{m}{C(s)} \right] = x_1 m \sum_i \mathrm{Res}\left(\frac{e^{st}}{C(s)}, s_i \right), \tag{26}$$

where, like $S_{RC}(t)$, only the poles from the characteristic polynomial $C(s)$ are involved. Such poles are clarified to the three cases as shown in Figure 3. Thus, we calculate $S_{RC}(t)$, $S_0(t)$ and $S_1(t)$ according to the following three cases.

Case i. $b^2 - 4mk < 0$

The poles are a pair of conjugated complex numbers $s_{3,4} = -\lambda \pm \mathrm{i}\mu$, where $\lambda = \frac{b}{2m}$ and $\mu = \frac{\sqrt{4mk-b^2}}{2m}$. By calculating the residues at the two simple poles $s_{3,4}$, we obtain

$$S_{RC}(t) = \frac{F\omega\left(b\sqrt{4mk-b^2}\cos(\mu t) + \left(b^2 - 2mk + 2m^2\omega^2\right)\sin(\mu t) \right)}{m^2\sqrt{4mk-b^2}\left(\lambda^4 + 2\lambda^2(\mu^2+\omega^2) + (\mu^2-\omega^2)^2 \right)} e^{-\lambda t}, \tag{27}$$

$$S_0(t) = x_0\left(\cos(\mu t) + \frac{b}{\sqrt{4mk-b^2}}\sin(\mu t) \right) e^{-\lambda t}, \tag{28}$$

$$S_1(t) = \frac{2x_1 m \sin(\mu t)}{\sqrt{4mk-b^2}} e^{-\lambda t}. \tag{29}$$

Case ii. $b^2 - 4mk > 0$

The poles are two negative real numbers $s_{3,4} = -\lambda \pm \nu$, where $\lambda = \frac{b}{2m}$ and $\nu = \frac{\sqrt{b^2-4mk}}{2m}$. By calculating the residues at the two simple poles $s_{3,4}$, we obtain

$$S_{RC}(t) = \frac{F\omega}{\sqrt{b^2-4mk}}\left(\frac{e^{-(\lambda-\nu)t}}{(\lambda-\nu)^2+\omega^2} - \frac{e^{-(\lambda+\nu)t}}{(\lambda+\nu)^2+\omega^2} \right), \tag{30}$$

$$S_0(t) = \frac{x_0}{2}\left(\left(1 + \frac{b}{\sqrt{b^2-4mk}} \right) e^{-(\lambda-\nu)t} + \left(1 - \frac{b}{\sqrt{b^2-4mk}} \right) e^{-(\lambda+\nu)t} \right), \tag{31}$$

$$S_1(t) = \frac{x_1 m}{\sqrt{b^2-4mk}}\left(e^{-(\lambda-\nu)t} - e^{-(\lambda+\nu)t} \right). \tag{32}$$

Case iii. $b^2 - 4mk = 0$

There is one second-ordered pole $s_3 = -\lambda = -\frac{b}{2m}$. By calculating the residues at the second-ordered pole s_3, we obtain

$$S_{RC}(t) = \frac{4Fm\omega\left(4bm + b^2t + 4m^2\omega^2t\right)}{\left(b^2 + 4m^2\omega^2\right)^2}e^{-\lambda t}, \tag{33}$$

$$S_0(t) = x_0(1+\lambda t)e^{-\lambda t}, \tag{34}$$

$$S_1(t) = x_1 te^{-\lambda t}. \tag{35}$$

In summary, the residue contribution from the sinusoidal excitation is a periodic oscillation in (24), whereas other solution components in Equations (27)–(35) all decay in negative exponential rates. We notice that the response to excitation, $S(t)$, is divided into two parts, $S_{RE}(t)$ and $S_{RC}(t)$. The former represents a steady periodic oscillation; the latter exhibits a negative exponential decay, respectively, in three patterns (27), (30), and (33).

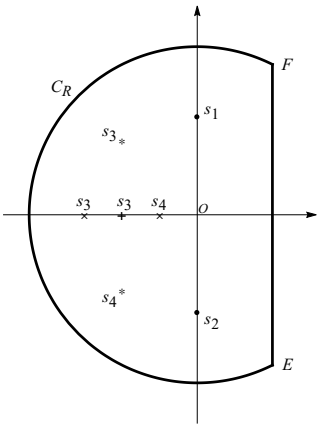

Figure 3. Contour in the integer-order case.

3.2. The Fractional Case $\alpha \in (0,1) \cup (1,2)$

In this case, the integral in (22) needs to be derived from a loop integral on the contour shown in Figure 4. Thus, in addition to the residue contribution, the Hankel integral contribution is added to the fractional case. For $S(t)$ in (22), the poles from the sinusoidal excitation are still $s_{1,2} = \pm i\omega$. For the fractional case, the poles from the characteristic polynomial $C(s) = ms^2 + bs^\alpha + k$ only have one case compared with the integer-order case $\alpha = 1$, that is, a pair of conjugated complex numbers with a negative real part on the principal Riemann sheet $-\pi < \arg s < \pi$ as shown in Figure 4 [19,29]. Denote the pair of simple poles by

$$s_{3,4} = -\lambda \pm i\mu = \eta e^{\pm i\phi}, \tag{36}$$

where $\lambda, \mu > 0$, $\eta = \sqrt{\lambda^2 + \mu^2}$ and $\phi = \pi - \arctan\frac{\mu}{\lambda}$.

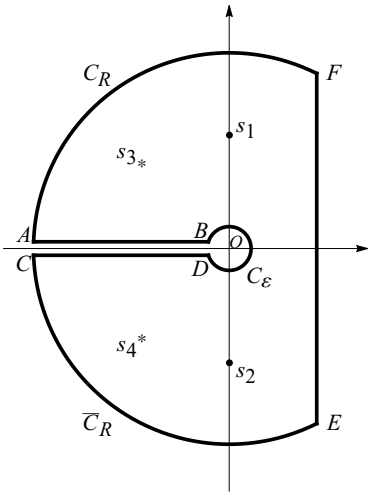

Figure 4. Contour in the fractional case.

By the residue theorem and Jordan's lemma, $S(t)$ in (22) is deformed to a sum of the residue contribution and the Hankel integral,

$$S(t) = S_R(t) + S_H(t), \tag{37}$$

where the residue contribution is further classified according to the origins of poles,

$$\begin{aligned} S_R(t) &= S_{RE}(t) + S_{RC}(t) \\ &= F\omega \sum_{i=1}^{2} \mathrm{Res}\left[\frac{e^{st}}{(s^2+\omega^2)C(s)}, s_i\right] + F\omega \sum_{i=3}^{4} \mathrm{Res}\left[\frac{e^{st}}{(s^2+\omega^2)C(s)}, s_i\right], \end{aligned} \tag{38}$$

and the Hankel integral is

$$S_H(t) = \frac{F\omega}{2\pi \mathrm{i}} \int_{\mathrm{Ha}} \frac{e^{st}}{(s^2+\omega^2)C(s)} ds, \tag{39}$$

where Ha denotes the Hankel loop encompassing the nonpositive real axis.

For (38), the residue contribution from the sinusoidal excitation is computed to be exactly the solution in Section 2 by using the Weyl fractional derivative

$$S_{RE}(t) = x_W(t), \tag{40}$$

while the residue contribution from the characteristic polynomial is computed as

$$\begin{aligned} S_{RC}(t) &= F\omega \left(\frac{e^{s_3 t}}{(s_3^2+\omega^2)C'(s_3)} + \frac{e^{s_4 t}}{(s_4^2+\omega^2)C'(s_4)} \right) \\ &= 2F\omega \,\mathrm{Re}\left(\frac{e^{(-\lambda+\mathrm{i}\mu)t}}{((-\lambda+\mathrm{i}\mu)^2+\omega^2)\left(2m(-\lambda+\mathrm{i}\mu)+b\alpha\eta^{\alpha-1}e^{\mathrm{i}(\alpha-1)\phi}\right)} \right) \\ &= \frac{2F\omega P\, e^{-\lambda t}}{\left(\lambda^4 + 2\lambda^2(\mu^2+\omega^2) + (\mu^2-\omega^2)^2\right)Q}, \end{aligned} \tag{41}$$

where $\mathrm{Re}(\cdot)$ denotes the real part and

$$\begin{aligned} P &= 2\eta^2\mu m\left(3\lambda^2 - \mu^2 + \omega^2\right)\sin(\mu t) + 2\eta^2\lambda m\left(-\lambda^2 + 3\mu^2 - \omega^2\right)\cos(\mu t) \\ &\quad -2\alpha b\lambda\mu\eta^{\alpha+1}\sin(\mu t - \alpha\phi + \phi) + \alpha b\eta^{\alpha+1}\left(\lambda^2 - \mu^2 + \omega^2\right)\cos(\mu t - \alpha\phi + \phi), \\ Q &= \alpha^2 b^2 \eta^{2\alpha} - 4\alpha b\lambda m\eta^{\alpha+1}\cos(\alpha\phi - \phi) + 4\alpha b\mu m\eta^{\alpha+1}\sin(\alpha\phi - \phi) \\ &\quad +4\eta^2\lambda^2 m^2 + 4\eta^2\mu^2 m^2. \end{aligned} \tag{42}$$

The Hankel integral in (39) is derived from the limit of an integral on the path $CD + C_\varepsilon + BA$ in Figure 4. The integral on the small circle C_ε approaches zero as follows

$$\lim_{\varepsilon\to 0^+} \frac{F\omega}{2\pi\mathrm{i}} \int_{C_\varepsilon} \frac{e^{st}}{(s^2+\omega^2)C(s)} ds = \lim_{\varepsilon\to 0^+} \frac{F\omega}{2\pi} \int_{-\pi}^{\pi} \frac{e^{\varepsilon t(\cos\theta + \mathrm{i}\sin\theta)}\varepsilon e^{\mathrm{i}\theta}}{(\varepsilon^2 e^{\mathrm{i}2\theta} + \omega^2)(m\varepsilon^2 e^{\mathrm{i}2\theta} + b\varepsilon^\alpha e^{\mathrm{i}\alpha\theta} + k)} d\theta = 0.$$

Thus, the Hankel integral in (39) becomes

$$\begin{aligned} S_H(t) &= -\frac{F\omega}{2\pi\mathrm{i}} \int_0^{+\infty} \frac{e^{-rt}}{r^2+\omega^2}\left(\frac{1}{C(re^{\mathrm{i}\pi})} - \frac{1}{C(re^{-\mathrm{i}\pi})}\right) dr \\ &= -\frac{F\omega}{\pi} \int_0^{+\infty} \frac{e^{-rt}}{r^2+\omega^2} \mathrm{Im}\left(\frac{1}{mr^2 + br^\alpha e^{\mathrm{i}\alpha\pi} + k}\right) dr \\ &= \frac{F\omega b \sin(\pi\alpha)}{\pi} \int_0^{\infty} \frac{r^\alpha e^{-rt}}{(r^2+\omega^2)V(r)} dr, \end{aligned} \tag{43}$$

where Im(·) denotes the imaginary part and

$$V(r) = b^2 r^{2\alpha} + 2b\cos(\pi\alpha)\left(k + mr^2\right)r^{\alpha} + k^2 + 2kmr^2 + m^2 r^4. \tag{44}$$

We checked whether α is taken as 1, the Hankel integral in (43) vanishes and $S(t)$ of the fractional case is simplified to that in Case i of Section 3.1. In Figure 5, the response $S(t)$ is shown for $m = 1$, $b = 2$, $k = 3$, $F = 1$, $\omega = 2$ and for different values of α. After excluding the steady periodic component $x_W(t)$, the curves of $S(t) - x_W(t)$ are shown in Figure 6. Under the zero initial value conditions, the transitions of responses to the steady state are displayed in Figure 5. From Figure 6, it can be observed that the decay in the case of $\alpha = 1$ is more rapid than the fractional cases.

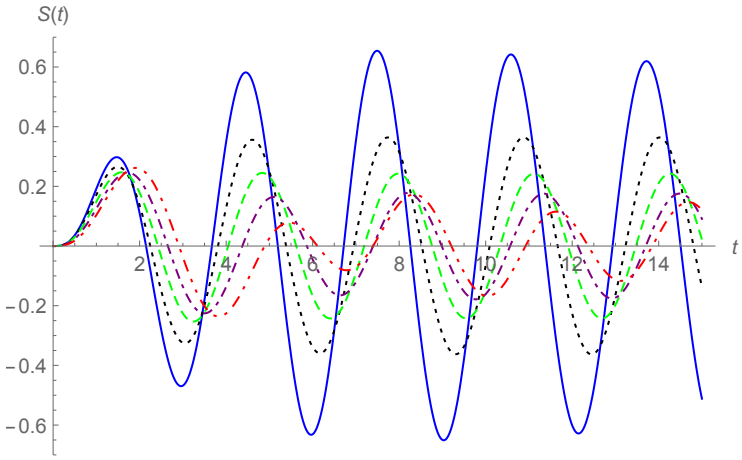

Figure 5. Response $S(t)$ for $\alpha = 0.3$ (solid line), $\alpha = 0.65$ (dot line), $\alpha = 1$ (dash line), $\alpha = 1.35$ (dot–dash line), $\alpha = 1.7$ (dot–dot–dash line).

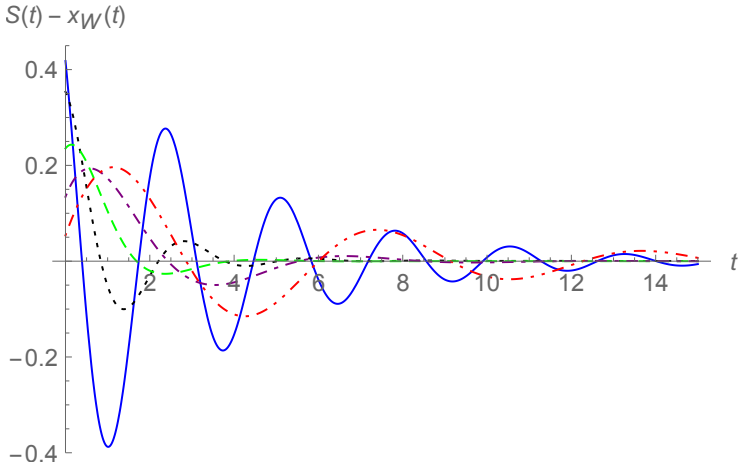

Figure 6. Curves of $S(t) - x_W(t)$ for $\alpha = 0.3$ (solid line), $\alpha = 0.65$ (dot line), $\alpha = 1$ (dash line), $\alpha = 1.35$ (dot–dash line), $\alpha = 1.7$ (dot–dot–dash line).

The two responses to initial values in (19) and (20) are computed in a similar manner. We list the results as follows

$$S_0(t) = S_{0R}(t) + S_{0H}(t), \tag{45}$$

$$S_{0R}(t) = x_0 \frac{2P_0 e^{-\lambda t}}{Q}, \tag{46}$$

$$S_{0H}(t) = \frac{x_0 bk\sin(\pi\alpha)}{\pi}\int_0^{\infty} \frac{r^{\alpha-1}e^{-rt}}{V(r)}dr, \tag{47}$$

$$S_1(t) = S_{1R}(t) + S_{1H}(t), \tag{48}$$

$$S_{1R}(t) = x_1 \frac{2P_1\, e^{-\lambda t}}{Q}, \tag{49}$$

$$S_{1H}(t) = \frac{x_1 b \sin(\pi\alpha)}{\pi} \int_0^\infty \frac{r^{\alpha-2}\left(mr^2 - \lceil \alpha - 1 \rceil (mr^2 + k)\right)}{V(r)} e^{-rt} dr, \tag{50}$$

where

$$\begin{aligned} P_0 &= \left(\alpha b^2 \eta^{2\alpha} + 2\eta^2 m^2 \lambda^2 + 2\eta^2 m^2 \mu^2\right) \cos(\mu t) - 2bm\eta^{\alpha+1}\lambda \cos(\mu t + \alpha\phi - \phi) \\ &\quad -\alpha bm\eta^{\alpha+1}\lambda \cos(\mu t - \alpha\phi + \phi) + 2bm\eta^{\alpha+1}\mu \sin(\mu t + \alpha\phi - \phi) - \alpha bm\eta^{\alpha+1}\mu \sin(\mu t - \alpha\phi + \phi), \\ P_1 &= 2\eta^2 \mu m^2 \sin(\mu t) - 2\eta^2 \lambda m^2 \cos(\mu t) + \lceil \alpha - 1 \rceil \alpha b^2 \eta^{2\alpha-1} \cos(\mu t - \phi) + \alpha bm\eta^{\alpha+1} \cos(\mu t - \alpha\phi + \phi) \\ &\quad -2\lceil \alpha - 1 \rceil b\lambda m\eta^{\alpha} \cos(\mu t + (\alpha - 2)\phi) + 2\lceil \alpha - 1 \rceil b\mu m\eta^{\alpha} \sin(\mu t + (\alpha - 2)\phi), \end{aligned}$$

Q and $V(r)$ are the same as in (42) and (44).

We checked that if α is taken as 1, the Hankel integrals in (47) and (50) vanish and the results of the fractional case for $S_0(t)$ and $S_1(t)$ are simplified to that in Case i of Section 3.1. Taking $m = 1$, $b = 2$ and $k = 3$, the responses $S_0(t)$ in Figure 7 and the responses $S_1(t)$ in Figure 8 are shown for $x_0 = 1$ and $x_1 = 1$, respectively, and for different values of α. From the two figures, more rapid decays in the case of $\alpha = 1$ are observed than that in the fractional cases.

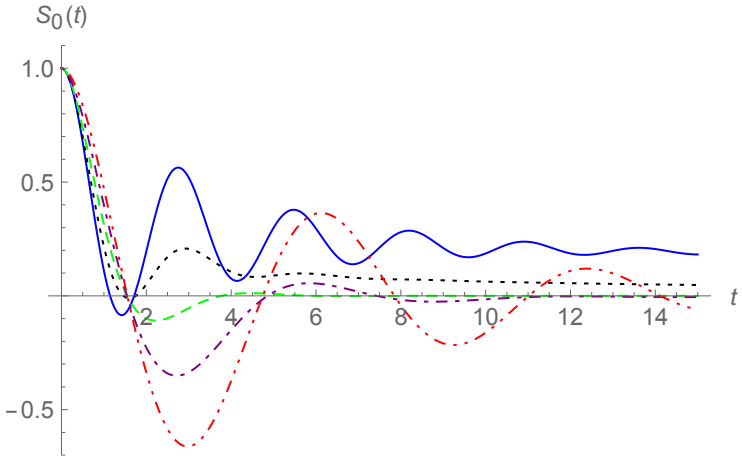

Figure 7. Response $S_0(t)$ for $\alpha = 0.3$ (solid line), $\alpha = 0.65$ (dot line), $\alpha = 1$ (dash line), $\alpha = 1.35$ (dot–dash line), $\alpha = 1.7$ (dot–dot–dash line).

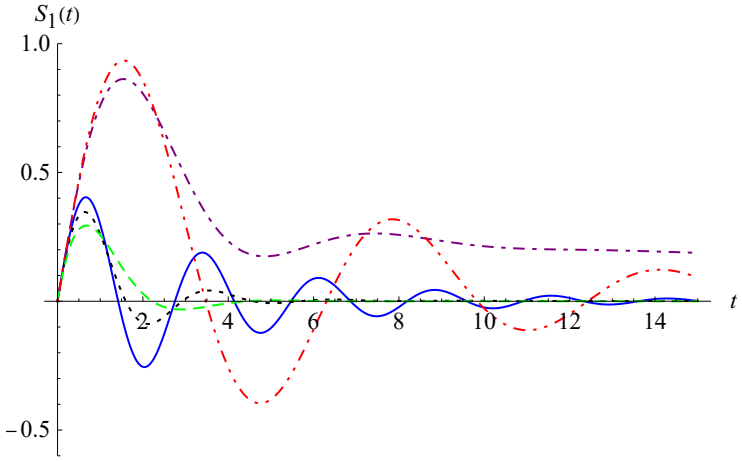

Figure 8. Response $S_1(t)$ for $\alpha = 0.3$ (solid line), $\alpha = 0.65$ (dot line), $\alpha = 1$ (dash line), $\alpha = 1.35$ (dot–dash line), $\alpha = 1.7$ (dot–dot–dash line).

In Figure 8, there is an abnormal jump between the curves of $\alpha = 1$ and $\alpha = 1.35$. In fact, $S_1(t;\alpha)$ is not right continuous with respect to the order α at the integer $\alpha = 1$. Specifically, $S_1(t;\alpha)$ at $\alpha = 1$ is

$$S_1(t;\alpha = 1) \quad = \quad x_1 \mathcal{L}^{-1}\left[\frac{m}{ms^2 + bs + k}\right],$$

however, the right limit of $S_1(t;\alpha)$ as $\alpha \to 1^+$ is

$$S_1(t;1^+) \quad = \quad x_1 \mathcal{L}^{-1}\left[\frac{m + bs^{-1}}{ms^2 + bs + k}\right],$$

from (20). Compared with (25), the right limit can be calculated as

$$S_1(t;1^+) \quad = \quad x_1 \int_0^t \frac{S_0(t;\alpha = 1)}{x_0} dt,$$

where $S_0(t;\alpha = 1)$ is given in Equations (28), (31) and (34) in Section 3.1. In Figure 9, a more detailed demonstration of $S_1(t)$ for $1 < \alpha < 2$ is shown, where α is taken as 1.2, 1.4, 1.6, and 1.8, and the right limit $S_1(t;1^+)$ is plotted by dot–dot–dash line.

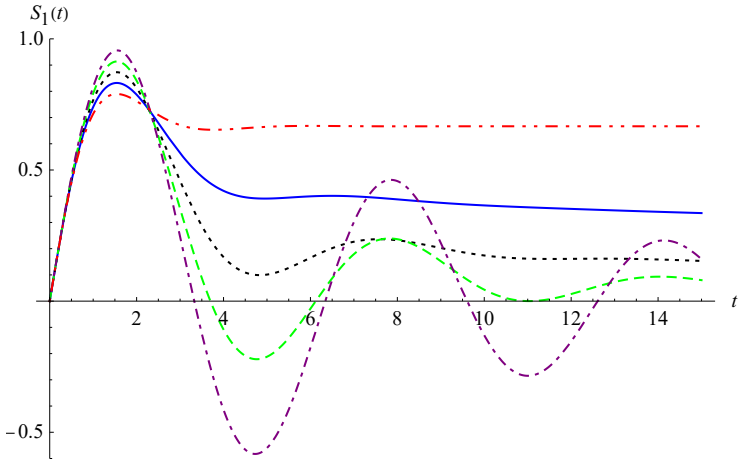

Figure 9. Response $S_1(t)$ for $\alpha = 1.2$ (solid line), $\alpha = 1.4$ (dot line), $\alpha = 1.6$ (dash line), $\alpha = 1.8$ (dot–dash line); the dot–dot–dash line is for the limit $S_1(t;1^+)$.

The curves in Figures 6–8 exhibit declines over time t. This can be made clear by looking into the asymptotic behaviors. First, we consider the Hankel integral contribution $S_H(t)$ in (43). Let $r = u/t$, and the integral in (43) is substituted as

$$S_H(t) = \frac{F\omega b \sin(\pi\alpha)}{\pi t} \int_0^\infty \frac{(u/t)^\alpha e^{-u}}{((u/t)^2 + \omega^2)V(u/t)} du. \tag{51}$$

As $t \to +\infty$, we have $V(u/t) \to k^2$, and hence the denominator of the integrand in (51) approaches to $k^2\omega^2$. Thus, we obtain the asymptotic representation for $S_H(t)$,

$$S_H(t) \sim \frac{Fb \sin(\pi\alpha)}{\pi k^2 \omega} t^{-\alpha-1} \int_0^\infty u^\alpha e^{-u} du = \frac{Fb \sin(\pi\alpha)\Gamma(\alpha+1)}{\pi k^2 \omega} t^{-\alpha-1}, \; t \to +\infty.$$

Considering the relationship $S(t) = x_W(t) + S_{RC}(t) + S_H(t)$, where $S_{RC}(t)$ decays in an oscillatory manner at a negative exponential rate, as a consequence, we obtain the asymptotic representation for the response to excitation

$$S(t) - x_W(t) \sim \frac{Fb \sin(\pi\alpha)\Gamma(\alpha+1)}{\pi k^2 \omega} t^{-\alpha-1}, \; t \to +\infty. \tag{52}$$

By a similar method, the two responses to the initial values have the asymptotic representations

$$S_0(t) \sim \frac{x_0 b \sin(\pi\alpha)\Gamma(\alpha)}{\pi k} t^{-\alpha},\ t \to +\infty, \tag{53}$$

$$S_1(t) \sim \begin{cases} \frac{x_1 bm \sin(\pi\alpha)\Gamma(\alpha+1)}{\pi k^2} t^{-\alpha-1},\ t \to +\infty,\ 0 < \alpha < 1, \\ -\frac{x_1 b \sin(\pi\alpha)\Gamma(\alpha-1)}{\pi k} t^{-(\alpha-1)},\ t \to +\infty,\ 1 < \alpha < 2. \end{cases} \tag{54}$$

By combining the above results in Equations (52)–(54), the asymptotic behavior of the solution of the initial value problem, (15) and (16), depends on the four cases of the initial values as follows.

Case A. $x_0 = 0, x_1 = 0$

$$x(t) - x_W(t) \sim \frac{Fb \sin(\pi\alpha)\Gamma(\alpha+1)}{\pi k^2 \omega} t^{-\alpha-1},\ t \to +\infty,$$

Case B. $x_0 \neq 0, x_1 = 0$

$$x(t) - x_W(t) \sim \frac{x_0 b \sin(\pi\alpha)\Gamma(\alpha)}{\pi k} t^{-\alpha},\ t \to +\infty,$$

Case C. $x_0 = 0, x_1 \neq 0$

$$x(t) - x_W(t) \sim \begin{cases} \frac{b \sin(\pi\alpha)\Gamma(\alpha+1)}{\pi k^2} (\frac{F}{\omega} + x_1 m) t^{-\alpha-1},\ t \to +\infty,\ 0 < \alpha < 1, \\ -\frac{x_1 b \sin(\pi\alpha)\Gamma(\alpha-1)}{\pi k} t^{-(\alpha-1)},\ t \to +\infty,\ 1 < \alpha < 2, \end{cases}$$

Case D. $x_0 \neq 0, x_1 \neq 0$

$$x(t) - x_W(t) \sim \begin{cases} \frac{x_0 b \sin(\pi\alpha)\Gamma(\alpha)}{\pi k} t^{-\alpha},\ t \to +\infty,\ 0 < \alpha < 1, \\ -\frac{x_1 b \sin(\pi\alpha)\Gamma(\alpha-1)}{\pi k} t^{-(\alpha-1)},\ t \to +\infty,\ 1 < \alpha < 2. \end{cases}$$

In summary, for the initial problem, (15) and (16), in the fractional case, we derive the response to excitation, $S(t)$, and the two responses to initial values, $S_0(t)$ and $S_1(t)$, and find that $S(t)$ is a superposition of a periodic oscillation $x_W(t)$, an exponentially decaying oscillation and a monotone recovery term in negative power law, and either $S_0(t)$ or $S_1(t)$ is a superposition of an exponentially decaying oscillation and a monotone recovery term in negative power law. The monotone recovery terms come from the Hankel integrals, and their attenuations in negative power laws dominate the exponential decays, which makes the fractional case different from the integer-order case. The steady periodic component $x_W(t)$ is just the response of the Weyl fractional oscillator in Section 2.

4. Conclusions

We consider the fractional oscillator equation with the fractional order $0 < \alpha < 2$ and the sinusoidal excitation, and conduct a comparative study of responses for the Weyl fractional derivative and the Caputo fractional derivative.

In Section 2, the fractional oscillator equation in the sense of Weyl is solved to be a steady periodic oscillation. The amplitude–frequency and the phase–frequency relations are analyzed with the variation of the order α. In Section 3, the fractional oscillator equation in the sense of Caputo subject to initial conditions is solved. For comparison, we first consider the integer-order case of $\alpha = 1$, and except for the steady periodic response, other solution components all decay in negative exponential rates. For the fractional case $\alpha \in (0,1) \cup (1,2)$, the response to excitation, $S(t)$, is a superposition of three parts: a steady periodic response in the sense of Weyl, an exponentially decaying oscillation, and a monotone recovery term in negative power law. For the two responses to initial values, $S_0(t)$ and $S_1(t)$, either of them is a superposition of an exponentially decaying oscillation and a monotone recovery term in negative power law. The monotone recovery terms come

from Hankel integrals, and their attenuations in negative power laws dominate over the exponential decays, which makes the fractional case different from the integer-order case. Finally, the asymptotic behaviors of the solutions removing the steady periodic response are given for the four cases of the initial values.

The Weyl fractional derivative is suitable for describing the steady-state problem, and can directly lead to a steady periodic solution. The Caputo fractional derivative is applied to an initial value problem, the method of the Laplace transform yields results and the steady component of the solution is just the solution of the corresponding Weyl fractional differential equation.

Author Contributions: Conceptualization, J.-S.D. and M.L.; Data curation, Y.-J.L. and M.L.; Formal analysis, J.-S.D., Y.-J.L. and M.L.; Funding acquisition, J.-S.D. and M.L.; Investigation, J.-S.D. and Y.-J.L.; Methodology, J.-S.D. and M.L.; Software, J.-S.D. and Y.-J.L.; Supervision, J.-S.D. and M.L.; Validation, M.L.; Visualization, J.-S.D. and Y.-J.L.; Writing—original draft, J.-S.D. and Y.-J.L.; Writing—review and editing, J.-S.D. and M.L. All authors have read and agreed to the published version of the manuscript.

Funding: This work was supported by the National Natural Science Foundation of China (Nos. 11772203; 61672238).

Institutional Review Board Statement: Not applicable.

Informed Consent Statement: Not applicable.

Data Availability Statement: Not applicable.

Conflicts of Interest: The authors declare no conflict of interest.

References

1. Miller, K.S.; Ross, B. *An Introduction to the Fractional Calculus and Fractional Differential Equations*; Wiley: New York, NY, USA, 1993.
2. Podlubny, I. *Fractional Differential Equations*; Academic: San Diego, CA, USA, 1999.
3. Kilbas, A.A.; Srivastava, H.M.; Trujillo, J.J. *Theory and Applications of Fractional Differential Equations*; Elsevier: Amsterdam, The Netherlands, 2006.
4. Mainardi, F. *Fractional Calculus and Waves in Linear Viscoelasticity*; Imperial College: London, UK, 2010.
5. Monje, C.A.; Chen, Y.Q.; Vinagre, B.M.; Xue, D.; Feliu, V. *Fractional-Order Systems and Controls, Fundamentals and Applications*; Springer: London, UK, 2010.
6. Băleanu, D.; Diethelm, K.; Scalas, E.; Trujillo, J.J. *Fractional Calculus Models and Numerical Methods. Series on Complexity, Nonlinearity and Chaos*; World Scientific: Boston, MA, USA, 2012.
7. Atanacković, T.M.; Pilipović, S.; Stanković, B.; Zorica, D. *Fractional Calculus with Applications in Mechanics*; Wiley: New York, NY, USA, 2014.
8. Li, M. *Theory of Fractional Engineering Vibrations*; De Gruyter: Berlin, Germany; Boston, MA, USA, 2021.
9. Diethelm, K. *The Analysis of Fractional Differential Equations*; Springer: Berlin/Heidelberg, Germany, 2010.
10. Bagley, R.L.; Torvik, P.J. On the fractional calculus model of viscoelastic behavior. *J. Rheol.* **1986**, *30*, 133–155. [CrossRef]
11. Lim, S.C.; Teo, L.P. The fractional oscillator process with two indices. *J. Phys. A Math. Theor.* **2009**, *42*, 065208. [CrossRef]
12. Li, M.; Sun, X.; Xiao, X. Revisiting fractional Gaussian noise. *Physica A* **2019**, *514*, 56–62. [CrossRef]
13. Samko, S.G.; Kilbas, A.A.; Marichev, O.I. *Fractional Integrals and Derivatives–Theory and Applications*; Gordon and Breach: Amsterdam, The Netherlands, 1993.
14. Palade, L.I.; Verney, V.; Attané, P. A modified fractional model to describe the entire viscoelastic behavior of polybutadienes from flow to glassy regime. *Rheol. Acta* **1996**, *35*, 265–273. [CrossRef]
15. Pritz, T. Five-parameter fractional derivative model for polymeric dampling materials. *J. Sound Vibr.* **2003**, *265*, 935–952. [CrossRef]
16. Duan, J.S.; Chen, Y.Q. Mechanical response and simulation for constitutive equations with distributed order derivatives. *Int. J. Model. Simul. Sci. Comput.* **2017**, *8*, 1750040. [CrossRef]
17. Achar, B.N.N.; Hanneken, J.W.; Enck, T.; Clarke, T. Dynamics of the fractional oscillator. *Physica A* **2001**, *297*, 361–367. [CrossRef]
18. Rossikhin, Y.A.; Shitikova, M.V. Application of fractional calculus for dynamic problems of solid mechanics: Novel trends and recent results. *Appl. Mech. Rev.* **2010**, *63*, 010801. [CrossRef]
19. Naber, M. Linear fractionally damped oscillator. *Int. J. Differ. Equat.* **2010**, *2010*, 197020. [CrossRef]
20. Wang, Z.H.; Du, M.L. Asymptotical behavior of the solution of a SDOF linear fractionally damped vibration system. *Shock Vib.* **2011**, *18*, 257–268. [CrossRef]

21. Liu, L.L.; Duan, J.S. A detailed analysis for the fundamental solution of fractional vibration equation. *Open Math.* **2015**, *13*, 826–838. [CrossRef]
22. Li, M. Three classes of fractional oscillators. *Symmetry* **2018**, *10*, 40. [CrossRef]
23. Wang, T.; Qin, M.; Lian, H. The asymptotic approximations to linear weakly singular Volterra integral equations via Laplace transform. *Numer. Algorithms* **2020**, *85*, 683–711. [CrossRef]
24. Duan, J.S.; Hu, D.C.; Li, M. Comparison of two different analytical forms of response for fractional oscillation equation. *Fractal Fract.* **2021**, *5*, 188. [CrossRef]
25. Dubovski, P.B.; Slepoi, J. Analysis of solutions of some multi-term fractional Bessel equations. *Fract. Calc. Appl. Anal.* **2021**, *24*, 1380–1408. [CrossRef]
26. Li, Y.; Duan, J.S. The periodic response of a fractional oscillator with a spring-pot and an inerter-pot. *J. Mech.* **2021**, *37*, 108–117. [CrossRef]
27. Duan, J.S.; Hu, D.C. Vibration systems with fractional-order and distributed-order derivatives characterizing viscoinertia. *Fractal Fract.* **2021**, *5*, 67. [CrossRef]
28. Shen, Y.J.; Yang, S.P.; Xing, H.J. Dynamical analysis of linear single degree-of-freedom oscillator with fractional-order derivative. *Acta Phys. Sin.* **2012**, *61*, 110505. [CrossRef]
29. Duan, J.S.; Zhang, Y.Y. Discriminant and root trajectories of characteristic equation of fractional vibration equation and their effects on solution components. *Fractal Fract.* **2022**, *6*, 514. [CrossRef]